

# Impact of Training Dataset Size on the Accuracy of L-SVR Single-Time-Point Renal Dosimetry for [<sup>177</sup>Lu]Lu-PSMA-617 Therapy

Abdurrahman Aziz Wicaksono<sup>1</sup>, Jaja Muhamad Jabar<sup>2</sup>, Syahril Siregar<sup>1</sup>, Deni Hardiansyah<sup>1\*</sup>

<sup>1</sup>Medical Physics and Biophysics, Physics Department, Faculty of Mathematics and Natural Sciences, Universitas Indonesia, Depok, Indonesia

<sup>2</sup>Nuclear and Biophysics, Physics Department, Faculty of Mathematics and Natural Sciences, Institut Teknologi Bandung, Bandung, Indonesia

Email: [\\*denihardiansyah@ui.ac.id](mailto:denihardiansyah@ui.ac.id)

Received: 1<sup>st</sup> December 2025; Revised: 16<sup>th</sup> December 2025; Accepted: 18<sup>th</sup> December 2025

**Abstract** – Radiopharmaceutical therapy (RPT) using [<sup>177</sup>Lu]Lu-PSMA-617 requires accurate dosimetry to evaluate organs-at-risk (OAR), specifically the kidneys. Single-time-point (STP) dosimetry simplifies clinical workflows by reducing SPECT/CT acquisition. Machine learning (ML) offers a potential solution, yet clinical implementation is hindered by the scarcity of sufficient training datasets for ML-based studies. This study investigated the relationship between training dataset size and time-integrated activity (TIA) estimation accuracy. A Linear Support Vector Regression (L-SVR) model was trained on synthetic virtual patients (VPs, 5,000 total) simulated from a published PBMS NLMEM renal biokinetics at five imaging times ( $t=1.8$  h, 18.7 h, 42.6 h, 66.2 h, and 160.3 h). Time-activity-curve (TAC) and reference TIA ( $rTIA$ ) were calculated for each VP. Random sampling was performed in increasing dataset sizes. Sample sizes were sub-sampled to training (80%) and testing (20%) datasets. L-SVR was trained on STP data at 42.6 h post-injection (best-time-point of PBMS NLMEM study) from the training dataset and tested by generating estimated TIA ( $eTIA$ ) with input from the testing dataset. Performance was evaluated by calculating root-mean-square-error (RMSE) and mean-absolute-percentage-error (MAPE) of the  $eTIA$  to  $rTIA$ . Results showed that the accuracy of  $eTIA$  from ML STP dosimetry depends on training size: small samples ( $n=10$ ) yielded poor performance ( $RMSE>85.98\%$ ,  $MAPE>89.1\%$ ). Accuracy improved significantly at  $n=500$  ( $RMSE=14.07\%$ ) and plateaued beyond  $n=1,000$  (peak  $RMSE=13.07\%$ ). Results indicate that the L-SVR model of the study requires sample sizes of  $n>200$ , with optimal gains up to  $n=2,000$ . This study suggests synthetic data as a methodological bridge between limited clinical datasets and data-intensive ML approaches.

**Keywords:** [<sup>177</sup>Lu]Lu-PSMA-617; Single-Time-Point dosimetry; Machine Learning; Support Vector Regression; Synthetic Data

## 1. Introduction

Radiopharmaceutical therapy (RPT) using [<sup>177</sup>Lu]Lu-PSMA-617 has shown considerable efficacy in treating various types of prostate cancer, including metastatic castration-resistant prostate cancer (mCRPC) [1-3]. Optimising treatment efficacy requires maximising tumour radiopharmaceutical uptake while sparing organs-at-risk (OAR), such as the kidneys. [4]. Dosimetry is a tool that allows the evaluation of radiopharmaceutical uptake, so that the estimation of absorbed doses on various targets and OARs may be performed. For example, determining radiation dose to the kidneys is considered to be important as it is considered the primary OAR in [<sup>177</sup>Lu]Lu-PSMA-617 therapy. The accuracy of such techniques relied heavily on the accuracy of the estimation of time-integrated activity (TIA), a parameter that represents the total number of radionuclide decays in any given target and OARs. [5]. The Medical Internal Radiation Dose (MIRD) formalism is the standard for clinical application of dosimetry, yet the challenge of serial quantitative imaging in a clinical setting for the estimation of TIA remained a hindrance for routine implementation.[6,7]. Reducing the number of required quantitative imaging would decrease operational burden and increase the likelihood of implementing individualised therapy. This is especially important for

nuclear medicine departments with limited inpatient capacity, imaging devices, qualified medical staff, and other factors that hinder implementation of therapy dosimetry.

To address these challenges, novel dosimetry methods, such as single-time-point (STP), were proposed as a potential solution to lower the workload for clinical dosimetry. Attempts have been made to develop methodologies, such as the study conducted by Hänscheid et al [8] and Madsen et al. [9], which are the frequently used STP methods in the literature. Hänscheid et al fitted a monoexponential decay model to biokinetic data to determine which model had the best accuracy given STP data. Madsen et al. mathematically derived a decay model and fitted biokinetic data to find an average population parameter to estimate TIA using STP data.

Machine learning (ML) has been proposed to offer the utility of learning complex biokinetics directly from data [10,11]. Recent development came from the study by Gomes et al [12], which introduced an STP method utilising Support Vector Regression (SVR) to predict effective half-life from a single scan time. They, however, did not highlight the challenge commonly faced in this type of study, which is the size of training data, and how it may impact TIA estimation accuracy. Statistical models, especially ones based on supervised training, develop better as they are given a large training dataset to minimise variance and overfitting, as shown in other fields [13-15]. Training on small cohorts carried the risk that the model would learn a narrow, patient-specific noise rather than population biokinetics. This limitation challenged the application of the model on a new patient population.

To determine the optimal sample size for clinical implementation, it is necessary to quantify the data requirements for ML-based dosimetry. This study was performed to systematically investigate the relationship between training dataset size on TIA estimation accuracy. It is hypothesised that estimation error will decrease as sample size increases, up to a point where additional training volume does not increase model performance considerably. To achieve said goal, this study employed a Linear Support Vector Regression (L-SVR) model trained on a large synthetic cohort of 5,000 virtual patients (VP), simulated based on a function derived from a population-based model selection non-linear mixed-effects model (PBMS NLMEM) from Hardiansyah et al. [16]. This method allows for a controlled analysis of how training dataset size influences TIA estimation accuracy, providing a landmark for future data collection that requires the application of ML in STP dosimetry.

## 2. Materials and Methods

### 2.1. PBMS NLMEM

The basis for simulating the virtual patient cohort was derived from an STP renal dosimetry study on [<sup>177</sup>Lu]Lu-PSMA-617 therapy, as reported by Hardiansyah et al.[16]. The study implemented population-based model selection with a non-linear mixed-effects model (PBMS NLMEM) on biokinetic data obtained from 63 patients with metastatic castration-resistant prostate cancer (mCRPC). The biokinetic data describe the radioactivity retention in the kidneys, measured by SPECT/CT imaging at five time points after injection, with the average imaging times after injection for the patient population as follows: TP1: 1.8 h, TP2: 18.7 h, TP3: 42.6 h, TP4: 66.2 h, and TP5: 160.3 h. The models were evaluated by goodness-of-fit and Akaike weight test, and the best performing model, as reported by the authors, was the four-exponential equation  $f_{6a}(t)$  and provided as Eq. 1:

$$f_{6a}(t) = A_1 e^{-(\lambda_1 + \lambda_{phys})t} + A_2 e^{-(\lambda_2 + \lambda_{phys})t} - A_3 e^{-(\lambda_3 + \lambda_{phys})t} - (A_1 + A_2 - A_3) e^{-(\lambda_{bc} + \lambda_{phys})t} \quad (1)$$

The time-integrated activity (TIA) may be obtained by analytically integrating Eq. 1 with respect to time from  $t = 0$  to  $t = \infty$ . The resulting analytical solution is given by eq. 2:

$$TIA = \int_0^{\infty} f_{6a}(t) dt = \left( \frac{A_1}{\lambda_1 + \lambda_{phys}} \right) + \left( \frac{A_2}{\lambda_2 + \lambda_{phys}} \right) - \left( \frac{A_3}{\lambda_3 + \lambda_{phys}} \right) - \left( \frac{A_1 + A_2 - A_3}{\lambda_{bc} + \lambda_{phys}} \right) \quad (2)$$

### 2.2. Software

The simulation of TAC, machine learning (ML) training, and performance evaluation workflows were implemented using the Python 3.13 programming language. Key libraries used in this study were: NumPy 2.1.3 for efficient numerical operations and array manipulation; scikit-learn 1.6.1 for implementing and training ML models, and matplotlib 3.10.0 for data visualisation and graphical analysis.

### 2.3. L-SVR

The ML model chosen for this study was the Linear Support Vector Regression (L-SVR) model. This model is highly efficient and scalable, which is appropriate for the needs of the study that required handling of large datasets. L-SVR avoids inefficient kernelization that may increase computational complexity, ensuring faster convergence and lower memory consumption during training [17,18]. This efficiency was essential to conduct the systematic performance analysis across increasingly large training set sizes.

### 2.4. Study Workflow

The study was structured into four main steps: virtual patient (VP) simulation, data preparation, ML training and prediction, and performance evaluation as shown in Fig 1.

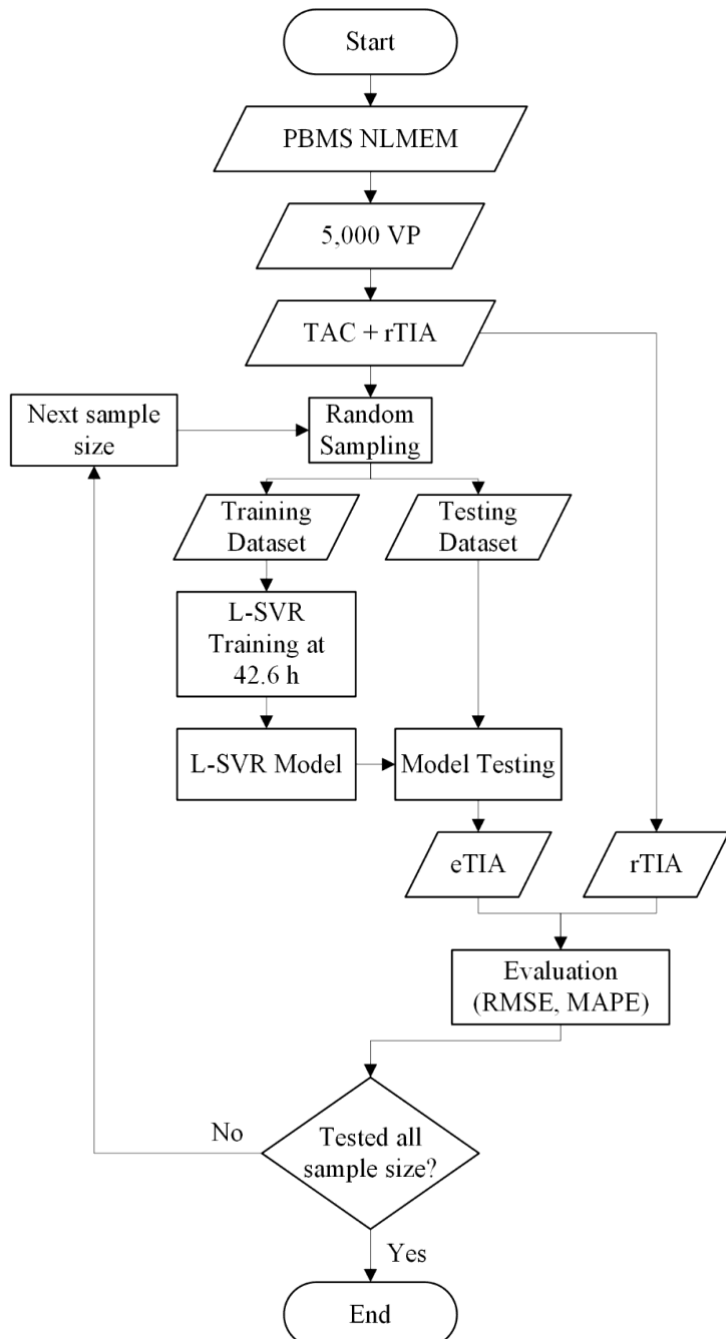


**Figure 1.** Flowchart of the Study

#### 2.4.1. Simulation

The simulation step involved generating a large synthetic dataset based on established PBMS NLMM exponential function (Eq. 1) and the reported distribution of the parameters (Table 2 of ref. [16]), stated as means and variances. The total number of VP generated was 5,000. Each VP corresponds to a single, randomly sampled set of the individual six biokinetic parameters defined in Eq 1. For each VP, Eq 1. was used to calculate the simulated activity values at five time-points post-injection (p.i.): TP1: 1.8 h, TP2: 18.7 h, TP3: 42.6 h, TP4: 66.2 h, and TP5: 160.3 h. The five activity values were simulated as a percentage of injected activity (%IA) and served as the input ML feature for the STP analysis. Substituting the parameters on all simulated TACs into the Eq. 2 will allow the calculation of the ground truth reference TIA (rTIA) for all VPs, which can serve as the target variable in ML training.

#### 2.4.2. Data Preparation

The large data matrix (5,000 VPs  $\times$  5 time points) was processed and sub-sampled to investigate the relationship between training size and model performance. To systematically evaluate the impact of training size, multiple reduced datasets were generated by performing random sampling on the following sample sizes:  $n = [10, 20, 50, 100, 200, 500, 1000, 2000, 5000]$ . To simulate clinical uncertainty that comes with SPECT/CT imaging (intra-individual variability), a random Gaussian error was added to the five simulated activity values for each VP. This noise was based on the fractional standard deviation (FSD) of 7.9% based on the published study [16]. The mathematical description of adding the error for the activity values was given in Eq. 3:

$$A_{noisy}(t) = A_{true}(t) \times (1 + FSD \times \mathcal{N}(0,1)) \quad (3)$$

Where  $A_{true}$  is the simulated activity without noise,  $A_{noisy}$  is the simulated activity with noise, and  $\mathcal{N}$  is a random number following a Gaussian distribution with a mean of 0 and a standard deviation of 1.

Each sub-sampled dataset was further split into a training dataset (80%) and a testing dataset (20%) [19,20]. This splitting of the sub-sampled dataset was repeated for every sample size step.

#### 2.4.3. Model Training

The L-SVR ML model was then trained iteratively across all sample sizes derived from the previous step. The model was trained using the noise-added STP activity values as input features and optimised to predict the corresponding rTIA. The trained model was then used to predict the eTIA for the remaining 20% of the sub-sampled dataset (test set). ML learning and performance evaluation of this study were performed for STP dosimetry at 42.6 h p.i., as it was reported that the PBMS NLMM performed best at this time-point [16].

#### 2.4.4. Performance Evaluation

The accuracy of the model was quantified by comparing the eTIA against the rTIA. The metric for comparing individual estimation accuracy was the relative deviation (RD), calculated as the fractional difference between eTIA and rTIA (Eq. 4):

$$RD = \frac{eTIA - rTIA}{rTIA} \times 100\% \quad (4)$$

Once the RD of all sub-sampled datasets were calculated, the overall performance of the ML model can be quantified by the performance metrics root mean square error (RMSE) and mean absolute percentage error (MAPE), as given in Eq. 5 and 6:

$$RMSE = \sqrt{SDRD^2 + (mean\ RD)^2} \quad (5)$$

$$MAPE = \frac{1}{n} \sum \left| \frac{eTIA - rTIA}{rTIA} \right| \times 100\% \quad (6)$$

In this study, eTIA with RD of over 20% were defined as outliers. This metric is relevant because low RMSE and MAPE values in the population may contain individuals with high RD values. This metric was shown as the number and percentages of eTIA relative to the size of the testing dataset above the following error thresholds: 5% (acceptable error), 10% (moderate error), and 20% (outliers).

### 3. Results

As detailed in Table 1, the model accuracy improved as the sample size increased, as can be seen by the drop in RMSE and MAPE. At small sample sizes ( $n = 10, n = 20$ ), the model showed poor estimation accuracy, with RMSE above 81% and MAPE above 71%. An inflection point can be seen as the training set size increased: from  $n = 20$  to  $n = 200$ , there is a sharp reduction in RMSE and MAPE, reducing from 81.02% to 17.44% and 78.51% to 13.54%, respectively. Beyond  $n = 200$ , however, estimation accuracy gains began to diminish. The metrics largely stabilised beyond  $n = 1000$ , suggesting a saturation point where additional training data may not increase estimation accuracy significantly. Sampling schedule at 42.6 was chosen to be viewed in Table 1 as evaluation showed that it has the best estimation accuracy based on RMSE, MAPE, and RD outlier analysis.

**Table 1.** Summary of performance metrics of the L-SVR model at 42.6 h

Sample Size (n)	RMSE	MAPE	RD>5% (#)	RD>5% (%)	RD>10% (#)	RD>10% (%)	RD>20% (#)	RD>20% (%)
10	85.98	89.1	2	100	2	100	2	100
20	81.02	78.51	4	99.95	4	99.85	4	100
50	63.12	52.16	10	98.62	10	97.24	9	93.33
100	35.05	26.43	19	93.54	17	86.89	14	66.67
200	17.44	13.54	32	78.96	23	58.18	9	25
500	14.07	11.73	73	73.35	49	49.35	17	14.67
1000	13.36	11.51	145	72.36	96	48.16	32	17.17
2000	13.14	11.51	290	72.39	191	47.87	63	14.58
5000	13.07	11.54	724	72.43	479	47.93	159	15.97

The impact of sample size was further analysed by evaluating the distribution of RD, particularly the reduction of estimation outliers. As shown in Fig 2, at low sample sizes, the estimations are highly unreliable, as nearly 100% of the estimations had RD of over 20% relative to the rTIA. Reliability improves as the sample size increases, as seen at  $n = 200$  where the proportion of outliers dropped to 14.58%. At  $n = 2000$ , the percentage of moderate errors reached a minimum of 47.87%, and outliers stabilised at 14.58%.

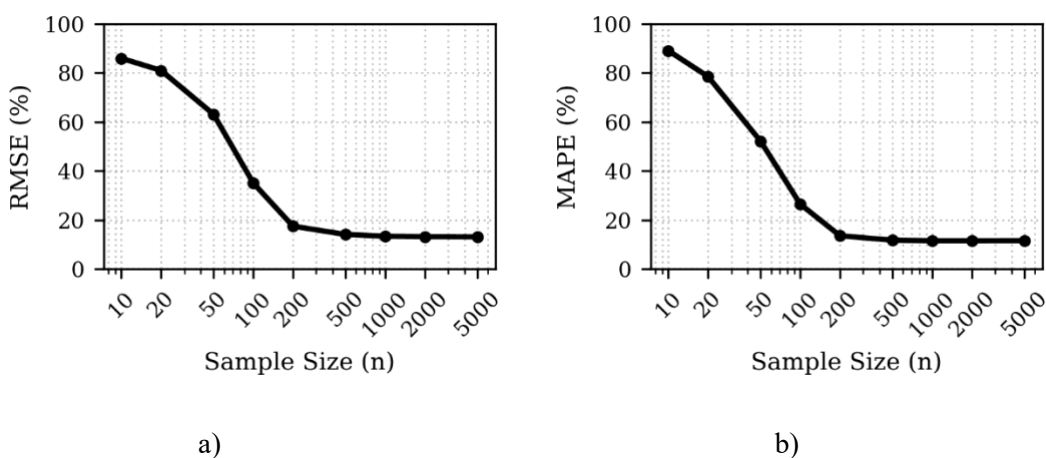


**Figure 2.** Learning curve graph of the L-SVR model at 42.6 h: a) showed the decrease of RMSE due to increasing sample size, and b) for MAPE, both in percentages.

Both the RMSE graph and MAPE graph exhibited similar decay in estimation error as the training set size increased. The model was shown to have a low error floor, stabilising at an RMSE of approximately 12-14%

#### **4. Discussion**

The main finding of this study is the importance of training dataset size, as the estimation accuracy of the L-SVR model has been shown to depend on the training dataset size. The sharp decrease in error (both RMSE and MAPE) observed between  $n = 50$  and  $n = 200$  indicated that a certain amount of data is required for the L-SVR model to adequately capture the relationships between STP data and the corresponding TIA. This finding showed that with a small sampling cohort, the reliability of ML training was lowered. The results of this study showed that with small sample sizes ( $n < 20$ ), the model failed to take into account underlying population variability, as reflected by RMSE exceeding 80%.

In addition to basic accuracy, analysing the outliers provided additional insight. As the sample size increased from 200 to 500, while the reduction of RMSE is about 3.37%, the number of outliers decreased by 10.33%. This implies that the unreliability of the model in small-cohort studies may be caused by a lack of data. It stands to reason that future attempts to integrate ML into a clinical dosimetry setting must incorporate an adequate volume of clinical dataset, and may be supplemented by synthetic data, as shown in this study, if required.

It was observed that the estimation accuracy at  $n = 5000$  was slightly lower than at  $n = 2000$  (slight increase of MAPE and estimations over RD thresholds). This small change in performance may be caused by stochastic variability in the error simulation rather than a true degradation of model performance. The reasoning behind this is that for  $n > 1000$  the quantification of the model performance reported values which are very close to each other, which implies the model is approaching an asymptotic limit to the model performance.

The practical challenges of recruiting over 2,000 patients for a single dosimetry study, the results of this study suggest that synthetic data and VPs may serve as a methodological aid. Given a reliable population model, generating large volumes of synthetic data that can be used for ML training is feasible. However, this method still inherently has limitations. The method, as outlined in this study, assumes that the biokinetic model used perfectly represents the population for which the model is used. The simulation assumes that imaging was performed at schedules exactly as it was defined, whereas in reality, actual scan times vary around a population average. Finally, the results of this study are limited to kidney dosimetry as the primary OAR of [ $^{177}\text{Lu}$ ]Lu-PSMA-617 therapy, as performance may be different for other organs or even tumour lesions. The performance of the L-SVR model in this study is promising, and may be improved further with the inclusion of additional patient-specific physiological or biomarker as input features that may capture inter-patient variability more comprehensively.

#### **5. Conclusion**

This study has shown that the accuracy of ML-based dosimetry depends on the training dataset size. An L-SVR model was trained on a large synthetic cohort of [ $^{177}\text{Lu}$ ]Lu-PSMA-617 renal dosimetry with STP data. Results showed that small-cohort datasets ( $n < 50$ ) are insufficient for capturing the population variability when using ML for calculating TIA with only biokinetic data as the input feature. The findings of this study suggest that increasing training size beyond 200 patients and up to about 2000 was associated with increased model performance. However, additional studies are required to validate these findings.

As it is challenging to recruit large patient cohorts, particularly in single-centre dosimetry studies, this study has shown the utility of implementing VPs to simulate synthetic data as a methodological bridge. It is proposed that future clinical dosimetry workflows may incorporate reliable population models to simulate large synthetic pre-training data, including patient-specific physiological or biomarker as input features for ML-based dosimetry methods in routine clinical practice.

#### **References**

- [1] S. Zhang, X. Wang, X. Gao, X. Chen, L. Li, G. Li, C. Liu, Y. Miao, R. Wang, K. Hu, Radiopharmaceuticals and their applications in medicine, *Signal Transduct. Target. Ther.* 10 (2025) 1. <https://doi.org/10.1038/s41392-024-02041-6>.
- [2] Y. Mirzaei, A. Hussein Mer, B. fattah Maran, L. Omidvar, F. Misamogooe, Z. Amirkhani, N. Javaheri Haghghi, N. Bagheri, Z. Keshtkar, B. Rezaei, F. Bargrizaneh, S. Jahandideh, N. Barpour, H. Shahsavaran, A. Bazyari, M. Abdollahpour-Alitappeh, *Clinical and preclinical advances in PSMA-*

Directed Antibody-Drug conjugates (ADCs): Current status and hope for the future, *Bioorganic Chem.* 153 (2024) 107803. <https://doi.org/10.1016/j.bioorg.2024.107803>.

[3] J. Fallah, S. Agrawal, H. Gittleman, M.H. Fiero, S. Subramaniam, C. John, W. Chen, T.K. Ricks, G. Niu, A. Fotenos, M. Wang, K. Chiang, W.F. Pierce, D.L. Suzman, S. Tang, R. Pazdur, L. Amiri-Kordestani, A. Ibrahim, P.G. Kluetz, FDA Approval Summary: Lutetium Lu 177 Vipivotide Tetraxetan for Patients with Metastatic Castration-Resistant Prostate Cancer, *Clin. Cancer Res.* 29 (2023) 1651–1657. <https://doi.org/10.1158/1078-0432.CCR-22-2875>.

[4] K. Herrmann, K. Rahbar, M. Eiber, R. Sparks, N. Baca, B.J. Krause, M. Lassmann, W. Jentzen, J. Tang, D. Chicco, P. Klein, L. Blumenstein, J.-R. Basque, J. Kurth, Renal and Multiorgan Safety of 177Lu-PSMA-617 in Patients with Metastatic Castration-Resistant Prostate Cancer in the VISION Dosimetry Substudy, *J. Nucl. Med.* 65 (2024) 71–78. <https://doi.org/10.2967/jnumed.123.265448>.

[5] S.R. Cherry, J.A. Sorenson, M.E. Phelps, *Physics in nuclear medicine*, 4th ed, Elsevier/Saunders, Philadelphia, 2012.

[6] M. Ljungberg, A. Celler, M.W. Konijnenberg, K.F. Eckerman, Y.K. Dewaraja, K. Sjögren-Gleisner, MIRD Pamphlet No. 26: Joint EANM/MIRD Guidelines for Quantitative <sup>177</sup>Lu SPECT Applied for Dosimetry of Radiopharmaceutical Therapy, *J. Nucl. Med.* 57 (2016) 151–162. <https://doi.org/10.2967/jnumed.115.159012>.

[7] W.E. Bolch, Y.K. Dewaraja, R.M. Bartlett, *MIRD Primer 2022: A Complete Guide to Radiopharmaceutical Dosimetry*, Society of Nuclear Medicine and Molecular Imaging, 2022.

[8] H. Hänscheid, C. Lapa, A.K. Buck, M. Lassmann, R.A. Werner, Dose Mapping After Endoradiotherapy with <sup>177</sup>Lu-DOTATATE/DOTATOC by a Single Measurement After 4 Days, *J. Nucl. Med.* 59 (2018) 75–81. <https://doi.org/10.2967/jnumed.117.193706>.

[9] M.T. Madsen, Y. Menda, T.M. O'Dorisio, M.S. O'Dorisio, Technical Note: Single time point dose estimate for exponential clearance, *Med. Phys.* 45 (2018) 2318–2324. <https://doi.org/10.1002/mp.12886>.

[10] W. Ding, J. Yu, C. Zheng, P. Fu, Q. Huang, D.D. Feng, Z. Yang, R.L. Wahl, Y. Zhou, Machine Learning-Based Noninvasive Quantification of Single-Imaging Session Dual-Tracer 18F-FDG and 68Ga-DOTATATE Dynamic PET-CT in Oncology, *IEEE Trans. Med. Imaging* 41 (2022) 347–359. <https://doi.org/10.1109/TMI.2021.3112783>.

[11] P. Kickingereder, D. Bonekamp, M. Nowosielski, A. Kratz, M. Sill, S. Burth, A. Wick, O. Eidel, H.-P. Schlemmer, A. Radbruch, J. Debus, C. Herold-Mende, A. Unterberg, D. Jones, S. Pfister, W. Wick, A. Von Deimling, M. Bendszus, D. Capper, Radiogenomics of Glioblastoma: Machine Learning-based Classification of Molecular Characteristics by Using Multiparametric and Multiregional MR Imaging Features, *Radiology* 281 (2016) 907–918. <https://doi.org/10.1148/radiol.2016161382>.

[12] C.V. Gomes, Y. Chen, I. Rauscher, S. Xue, A. Gafita, J. Hu, R. Seifert, L. Mercolli, J. Brosch-Lenz, J. Hong, M. Ryhiner, S. Ziegler, A. Afshar-Oromieh, A. Rominger, M. Eiber, T.V.M. Lima, K. Shi, Characterization of Effective Half-Life for Instant Single-Time-Point Dosimetry Using Machine Learning, *J. Nucl. Med.* (2025). <https://doi.org/10.2967/jnumed.124.268175>.

[13] A. Bailly, C. Blanc, É. Francis, T. Guillotin, F. Jamal, B. Wakim, P. Roy, Effects of dataset size and interactions on the prediction performance of logistic regression and deep learning models, *Comput. Methods Programs Biomed.* 213 (2022) 106504. <https://doi.org/10.1016/j.cmpb.2021.106504>.

[14] D. Rajput, W.-J. Wang, C.-C. Chen, Evaluation of a decided sample size in machine learning applications, *BMC Bioinformatics* 24 (2023) 48. <https://doi.org/10.1186/s12859-023-05156-9>.

[15] J.G.A. Barbedo, Impact of dataset size and variety on the effectiveness of deep learning and transfer learning for plant disease classification, *Comput. Electron. Agric.* 153 (2018) 46–53. <https://doi.org/10.1016/j.compag.2018.08.013>.

[16] D. Hardiansyah, E. Yousefzadeh-Nowshahr, F. Kind, A.J. Beer, J. Ruf, G. Glatting, M. Mix, Single-Time-Point Renal Dosimetry Using Nonlinear Mixed-Effects Modeling and Population-Based Model Selection in [ <sup>177</sup> Lu]Lu-PSMA-617 Therapy, *J. Nucl. Med.* (2024) jnumed.123.266268. <https://doi.org/10.2967/jnumed.123.266268>.

[17] A.J. Smola, B. Schölkopf, A tutorial on support vector regression, *Stat. Comput.* 14 (2004) 199–222. <https://doi.org/10.1023/B:STCO.0000035301.49549.88>.

[18] O.L. Mangasarian, D.R. Musicant, Robust linear and support vector regression, *IEEE Trans. Pattern Anal. Mach. Intell.* 22 (2000) 950–955. <https://doi.org/10.1109/34.877518>.

- [19] R. Medar, V.S. Rajpurohit, B. Rashmi, Impact of Training and Testing Data Splits on Accuracy of Time Series Forecasting in Machine Learning, in: 2017 Int. Conf. Comput. Commun. Control Autom. ICCUBEA, 2017: pp. 1–6. <https://doi.org/10.1109/ICCUBEA.2017.8463779>.
- [20] R.A. Bauder, T.M. Khoshgoftaar, Medicare Fraud Detection Using Machine Learning Methods, in: 2017 16th IEEE Int. Conf. Mach. Learn. Appl. ICMLA, 2017: pp. 858–865. <https://doi.org/10.1109/ICMLA.2017.00-48>.